

## A new approach to function-structure modeling of the surface modified polymers

Fedor A. Doronin<sup>1,a</sup>, Andrey G. Evdokimov<sup>1,b</sup>, Yury V. Rudyak<sup>1,c</sup>, Georgy O. Rytikov<sup>1,2,d</sup>,  
Irina P. Taranets<sup>1,e</sup>, Viktor G. Nazarov<sup>1,f</sup>

<sup>1</sup>Moscow Polytechnic University, Moscow, Russia

<sup>2</sup>State university of management, Moscow, Russia

<sup>a</sup>f.a.doronin@mospolytech.ru, <sup>b</sup>evdokag@gmail.com, <sup>c</sup>rudyak@mail.ru, <sup>d</sup>gr-yandex@yandex.ru,

<sup>e</sup>qwerty818@mail.ru, <sup>f</sup>110505n@gmail.com

Corresponding author: Fedor A. Doronin, f.a.doronin@mospolytech.ru

PACS 87.15.Aa

**ABSTRACT** We introduce a novel approach to function-structure modeling of the polymer materials. It's based on mathematical and statistical processing of the images obtained by scanning electron microscopy (SEM) of the corresponding surfaces. We studied the correlation-rotational anisotropy, the degrees of planar and contour heterogeneity and the morphological spectra of the SEM images to characterize the function-structure relationships quantitatively. The introduced quantitative characteristics will allow to rationalize the choice of chemical compositions of the modifying gas mixtures (for example, helium-fluorine-oxygen) that provide the maximum possible wetting edge angles for the materials under consideration with reference polar and non-polar liquids.

**KEYWORDS** oxyfluorination, scanning electron microscopy, modification, morphology, correlation, polymer substrate

**ACKNOWLEDGEMENTS** This work was carried out with the financial support of the Ministry of science and higher education of the Russian Federation (State assignment "Structure and properties of polymer materials obtained with the use of systems of methods of chemically, thermally and / or mechanically induced surface and volume modification", topic number FZRR-2020-0024, code 0699-2020-0024).

**FOR CITATION** Doronin F.A., Evdokimov A.G., Rudyak Yu.V., Rytikov G.O., Taranets I.P., Nazarov V.G. A new approach to function-structure modeling of the surface modified polymers. *Nanosystems: Phys. Chem. Math.*, 2022, **13** (1), 115–127.

### 1. Introduction

Surface modification of the polymers is a well-known method for altering their physical, chemical and functional characteristics [1–3]. Classifying the methods of the surface modification by the aggregate state of the modifier, we can conditionally distinguish solid-, liquid- and gas-phase approaches to the surface treatment [4–6]. There are also a number of additional activation techniques: mechanical, thermal, electro- and optical methods [7–11]. In particular, gas-phase oxyfluorination allows the formation of heterogeneous coatings with different chemical and morphological design and thus with a wide range of controlled set of physical, chemical and, as a result, functional surface properties. This is possible due to the synergetic cooperation of the optimal gas mixture composition and the external factors (temperature, pressure) acting during the processing [12–18] on the surface of commonly used polymers (such as low-density polyethylene (LDPE), polypropylene (PP), polyethyleneterephthalate (PET), etc.). Considering the development trends in the direction of "personalized" production of polymers and their compositions for the private scientific-technical and production tasks using surface, bulk, additive and combined modification techniques [19–23], adjusting the ratio of (for example, in the case of oxyfluorination) the gas mixture components that provides the functional-operational properties specifications for the manufactured polymer products becomes more complicated. It is obvious that the set of polymer properties formed in the process of modification occurs both due to changes in their chemical composition and structure and due to micro- and nanotexturing of the corresponding surfaces [24–28]. In particular, under the manufacturing of the polymer-based composite materials with reduced platelet adhesion (for medical purposes), it was shown that the plasma-chemical treatment, the sulfation or the fluorination can provide a radical reduction in the thrombocyte activation and in the platelet adhesion to the modified LDPE-surface [29]. Micro- and nanotextures formed on the polymer surface during the modification affect surface parameters such as friction coefficients, wettability (hydrophilicity/hydrophobicity) and adhesion [30–34]. One of the main high-precision tools for polymer surface morphology (in the mode of secondary electrons scattering) and chemical composition (in the mode of energy-dispersion analysis) studying is scanning electron microscopy (SEM) [35, 36] that provides an ultimate spatial resolution of the generated images in range from 1 to 10 nm. However, along with the high technical capabilities of the scanning electron microscope, it can not be considered as a

“reference” and fully reliable way to study surfaces because, when adjusting the contrast and brightness, the microscope-operators are often guided by their own subjective visual perception of the analyzed image. And moreover, as a rule, they try to visualize the exotic features (artifacts) of the studied surface and pay insufficient attention to the quantitative analysis of the background textures that, in most cases, determine the macro- and nanoscopic properties of the studied objects [37–39]. It is obvious that shooting the same object under various conditions can lead to completely different conclusions about the true morphology and structure of its surface (Fig. 1).

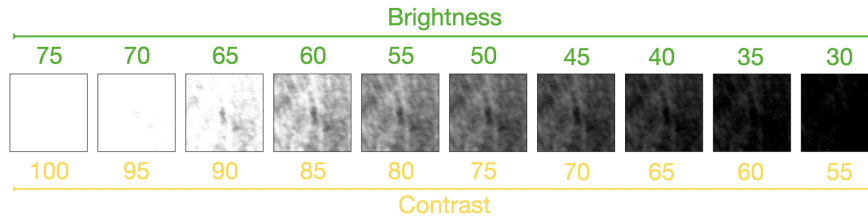


FIG. 1. The SEM image [40] of the same LDPE-film at different values of image brightness and contrast

Visual analysis of the SEM-image pictures with 75, 70 and 30 % of brightness shows that the film of low-density polyethylene (LDPE) is homogeneous and does not have an explicit texture. However, pictures with brightness levels from 65 to 45 % demonstrate the presence of a well-developed, most likely, multi-modal system of morphological inhomogeneities. Similar problems of obtained results interpretation are usually encountered in medicine under the visual analysis of ultrasound studies, x-rays and optical images in order to diagnose and monitor the dynamics of various diseases [41–46].

The most modern analytical devices designed to study the surfaces of polymers and other materials have specialized software and hardware complexes (set-top boxes), which include digital tools for the formed surface images processing. In particular, atomic force microscopes can form three-dimensional surface images and provide information about the average values of a number of quantitative roughness characteristics ( $R_a$ ,  $R_q$ ,  $S_m$ , etc. [47–51]). Thus, in [52], the morphology and roughness parameters of fluorinated films of polyvinylchloride (PVC) and polyethyleneterephthalate (PET) were investigated using atomic force microscopy (Fig. 2).

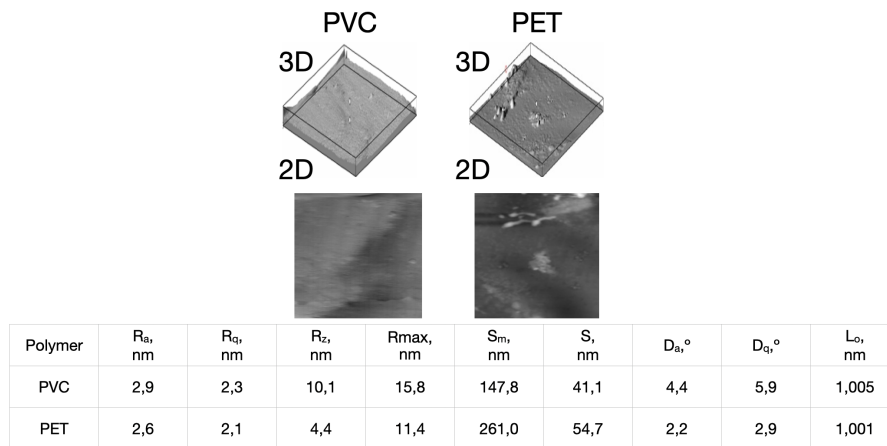


FIG. 2. The AFM-images of the surface fragments of the fluorinated PVC- and PET-films [52]

It can be seen that the undulation of the surface of the fluorinated PVC-sample is formed by single nanoscale “protrusions” ( $R_a \sim 3$  nm) and extended “folds”, the characteristic transverse dimensions of which ( $S \sim 40$  nm) are significantly inferior to the longitudinal ones ( $S_m \sim 150$  nm). Both “folds” ( $S \sim 50$  nm and  $S_m \sim 260$  nm) and single “protrusions” ( $R_a \sim 3$  nm) are also observed on the surface of the PET-sample. The Pearson correlation coefficient calculated for the two presented sets of nanorelief characteristics is  $\sim 0.997$ , which indicates the textural homogeneity (high degree of similarity of surface nanotextures) of the films under consideration. But the values of the free surface energy of the modified PET- and PVC-samples differ and are 90 [53] and 50 [54] mN/m respectively, which is probably due to the chemical nature of the materials under discussion. Another important example for understanding the considering problem is presented in [55]. Fig. 3 shows three SEM-images of the surfaces fragments of different LDPE-films produced under the same industrial technology.

Taking into account the widely known large dispersion of the contact angle of wetting values for the chemically identical samples ( $\pm 10^\circ$ ), easily visually observable morphological features of the textures (Fig. 3) can make a significant

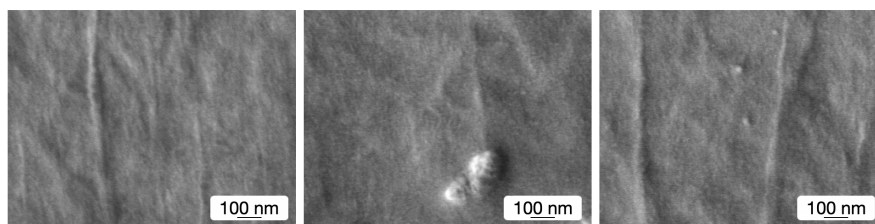


FIG. 3. The SEM-images of the surface fragments of unmodified (initial) LDPE-films [55]

contribution to the formation of free surface energy values, which in particular, determines the characteristics of the surface wetting. But when predicting the main macroscopic physical and chemical properties of chemically identical polymer matrices, it is necessary to focus on the textural characteristics of such areas where the single macroscopic defects (microcracks, microcrystals of third-party substances, fibers, etc.) are not observed. Thus, it is important to choose a rational zone for nanoscopic (SEM, AFM, EDS, etc.) analysis, since most of the studied polymer substrates are characterized by a certain level of initial defects which is not associated with modifying external influences. In connection with the above, to effectively design and predict the properties of the modified materials based on the quantitative analysis of their surfaces SEM-images it is necessary: – to conduct the additional studies of the of polymer films' chemical structure that can be performed, for example, with the scanning electron microscopy in the mode of the EDS-analysis; – to develop more sensitive techniques for the specification of the digital nanorelief models' parameters that would allow us to statistically reliably distinguish the samples with different physical and chemical properties. Thus, the quantitative analysis of images of polymer surfaces (in particular, SEM-images) becomes extremely important, first, in order to reduce the dependence of the observation results on the operators of measuring complexes, and, second, in order to provide the possibility of introducing quantitative measures, criteria and techniques that allow comparing nanotextures of the surfaces (in particular, for the fluoropolymers) previously observed under approximately the same conditions [56]. The original concepts and techniques for applying some possible solutions to the problem of quantitative description and modeling of polymer film surface structures are presented in [57].

In the framework of the present paper, two algorithms of computer analysis were developed for the texture deficiency of the polymeric substrates surfaces (for example, LDPE). The algorithms are based on the quantitative determination of the characteristic size of the morphological spectrum localization region and of the rotational anisotropy degrees of the characteristic functions of the corresponding SEM-images digital heterogeneities. Based on the information about the features of the nanorelief surfaces of LDPE-samples, a retrospective assessment of the optimality of the chemical compositions of the modifying mixture used in their gas-phase treatment with the oxyfluorination technique.

## 2. Material and methods

Some polymer material surface modification methods (e.g., fluorination, sulfonation, corona discharge treatment, etc.) were considered in [58, 59]. The most impressive achievement is that of the surface superhydrophilicity for a number of initially hydrophobic polymers that was demonstrated in [59] as a consequence of the oxyfluorination – the gas-phase modification of the samples by mixtures of helium, fluorine and oxygen. The surface oxyfluorination of the LDPE-films (NPO Plastik, Russia) was performed in a 500 ml stainless steel reactor with preliminary and subsequent vacuuming according to the method [59] at four concentrations of gas mixture components: 1) 7%F<sub>2</sub>/10%O<sub>2</sub>/83%He; 2) 10%F<sub>2</sub>/6%O<sub>2</sub>/84%He; 3) 11%F<sub>2</sub>/4%O<sub>2</sub>/85%He; 4) 15%F<sub>2</sub>/~0.5%O<sub>2</sub>/84.5%He (the ~ 0.5 % concentration of O<sub>2</sub> is due to its content in industrially diluted F<sub>2</sub>). The processing times for the LDPE-films were 5, 30 and 180 minutes. The morphological changes of the LDPE-films surfaces before and after the modification were monitored using the autoemission scanning electron microscope JSM 7500-F ("JEOL", Japan) operated at an accelerating voltage of 10 kV. The achieved spatial resolution was ~ 1 nm. To reduce the level of static charge and to prevent the destruction of dielectrics under the action of an electron beam, a pre-sputtering layer of platinum (~ 8 nm thickness) was superimposed on the samples' surfaces. In Fig. 4 the results of the morphological structure investigation for the LDPE-films surfaces (3 series for each modification mode) with the scanning electron microscopy in the mode of secondary electron scattering are shown.

The visual analysis of the presented SEM images suggests that the largest number of nanoobjects (light spots) of approximately the same size (1 – 10 nm) formed during the oxyfluorination is observed at a certain optimal ratio of fluorine and oxygen concentrations in the modifying gas mixture. It is also clearly visible that the particular implementations of the LDPE-films surfaces' textures differ significantly from each other. However, the physico-chemical properties of the discussed surfaces (the wettability, the permeability, the sorption capacity, the work of adhesion, etc.) are the same for all private implementations obtained under the same conditions of the oxyfluorination, and they significantly depend on the composition of the modifying gas mixture due to the dissimilar values of the modified LDPE-films' free surface energies derived under the different oxyfluorination modes. The quantitative estimation of free surface energy value can,

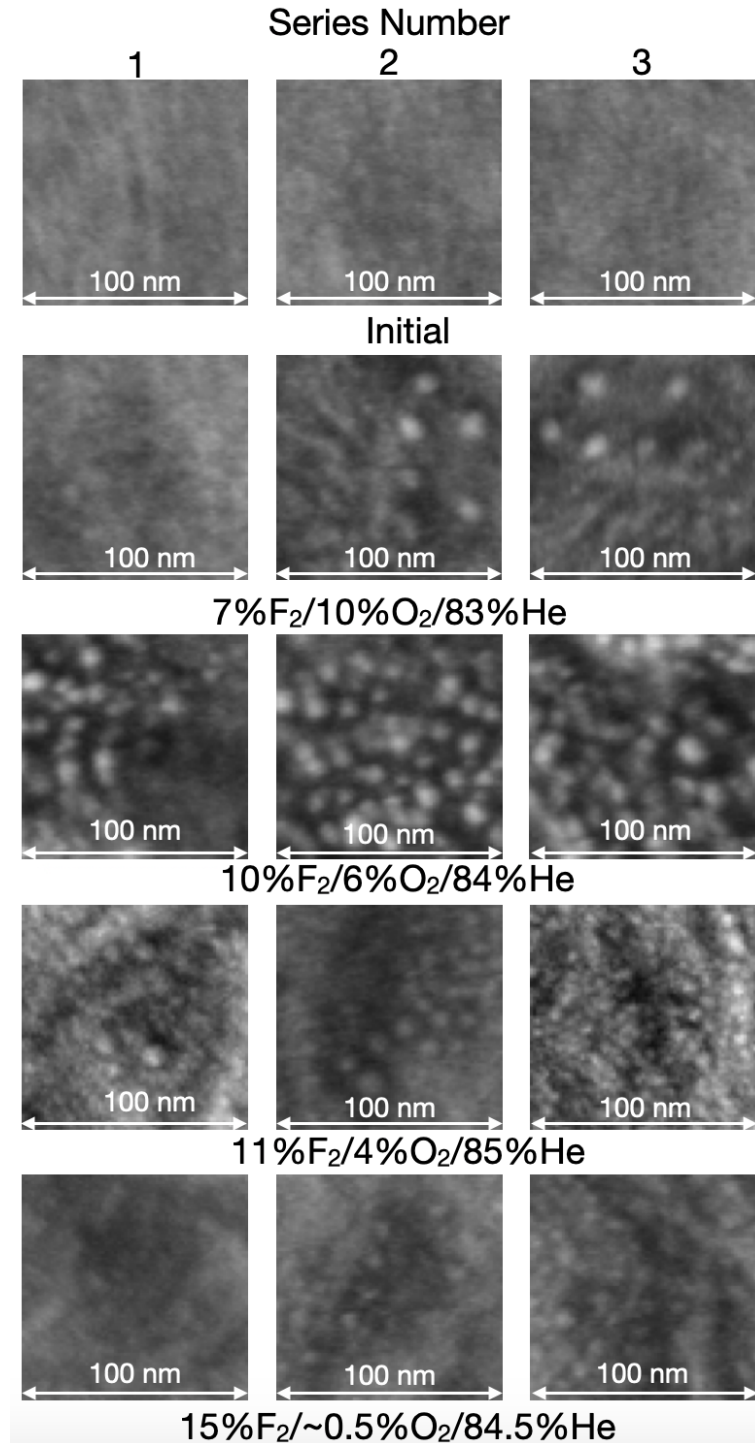


FIG. 4. The SEM-images of the oxyfluorinated LDPE samples (the characteristic size (square side) of the analyzed regions  $\sim 100$  nm)

in particular, be carried out on the basis of direct macroscopic measurements of the wetting edge angles with reference polar (distilled water) and less-polar (ethylene glycol) liquids. The determination of the LDPE films edge wetting angle with the distilled water and the ethylene glycol “before” and “after” the modification procedures was carried out on an upgraded laboratory stand for high-speed micro-photography of the wetting process in the photo/video fixation mode [56]. The obtained results are shown in Table 1.

Thus, there is a need for internally-consistent quantitative characterization of the textures of both individual LDPE-samples and the corresponding series as a whole. This requires implementation of a rational parameterization and the design of such a texture simulation approach that, on one hand, differs the individual samples from each other, and on another, gives the common model to the series.

TABLE 1. The edge wetting angles for the LDPE-substrates oxyfluorinated under the various modification modes

Free Surface Energy, mJ/m <sup>2</sup>	$\Theta_w, ^\circ$	$\Theta_e, ^\circ$	He, %	F <sub>2</sub> , %	O <sub>2</sub> , %
27 ± 3	78 ± 8	63 ± 6	—	—	—
46 ± 5	54 ± 5	22 ± 2	83 ± 1	7.0 ± 0.5	10.0 ± 0.5
44 ± 4	57 ± 6	28 ± 3	84 ± 1	10.0 ± 0.5	6.0 ± 0.5
46 ± 5	54 ± 5	32 ± 3	85 ± 1	11.0 ± 0.5	4.0 ± 0.5
41 ± 4	67 ± 7	34 ± 3	84.5 ± 0.5	15.0 ± 0.5	0.5 ± 0.5

### 3. Results and the discussion

#### 3.1. The correlation-rotational anisotropy of the polymer surfaces SEM-images

The probability that a random defect will take the form of an object that has a symmetry is quite small. Such defects usually attract researchers' attention and the theory of their genesis, formation and potential practical applications appears quickly. As it was shown in the "Introduction" section, when predicting the properties of macroscopically homogeneous polymer films, it is necessary to focus on the "defect-free" or "low-defect" areas of the surfaces. It is evident that any initial images show areas that are more or less optically homogeneous. The more that a secondary image (formed by rotating the initial one to an arbitrary angle) differs from the primary one, the more optically heterogeneous it is. Thus, any observed defects demonstrate a high level of the rotational optical anisotropy, which does not allow us to consider such areas as representative in further analysis. While the "defect-free" and the "low-defect" zones provide a relatively high level of rotational correlation and a low level of rotational anisotropy. The modified LDPE-samples do not contain obvious macroscopic defects (Fig. 4), but the mesoscopic defects can be masked as regular inhomogeneities of the nanorelief. So it was necessary to develop an algorithm for automatic selection for further analysis of areas that are characterized by the greatest observed structural homogeneity. The post-rejection of the samples with the microcracks, agglomerates of foreign particles, fibers and etc. will significantly improve the quality of the analytic data obtained by the researchers from measuring devices characterized by (potentially) nanoscopic resolution in the future. A scanning electron microscope operating in the mode of secondary electron scattering is usually used as a nanorelief visualizer. The characteristic geometric dimensions of the vertical inhomogeneities of the studied textures can be associated with the polymer film surfaces images pixels' brightnesses expressed in relative units (nanorelief indices) in accordance with the device intrinsic algorithms. Thus, the quantitative SEM-image analysis allows us to create the digital models of the investigated surfaces that can be used to carry out the structural and functional properties forecasting (in particular, for the oxyfluorinated polymers) in the future. Fifteen primary digital images were generated from the corresponding SEM-images by tabulating the values of the corresponding pixels' brightnesses (five series of three digital images each). Using the standard rotation transformations of the coordinate system, 9 secondary images were obtained from the primary digital images (the rotation was performed in the range from 0° to 90° with a step of 10°). By averaging the numerical values of the corresponding pixel brightness, five statistical digital models of the studied surfaces were formed. For each of them the maximum and minimum values of the nanorelief indexes were found. Their dependences on the fluorine and oxygen concentrations are shown in Fig. 5. Based on the results obtained (Fig. 6), it can be assumed that the presence of significant changes in the functional properties of the modified LDPE-films could be observed when a gas mixture was ~ 13%F<sub>2</sub>/~ 3%O<sub>2</sub>/~ 84%He. At the specified concentrations of active components of the modifying mixture, local extremes of the minimum and maximum values of the corresponding nanorelief indices are observed.

#### 3.2. The digital morphological heterogeneity of the polymer surfaces SEM-images

It was shown in [57] that for characterization of the surfaces' digital images it is possible to use several quantitative measures describing different aspects of forming pictures pixels' brightnesses inhomogeneities. In particular, it was found that the efficient parameters are:

- the "planar heterogeneity"  $\sigma = S/S_0$ , where  $S$  – the total area of flat shapes with a brightness less than the "threshold" value  $A_0$ ; the  $S_0$  – the area of the entire image. To calculate  $\sigma$ , the "threshold"  $A_0$  takes in turn all natural values from the interval [0; 255] from minimum brightness to maximum brightness.

- the "contour heterogeneity"  $\lambda = L/L_0$ , where  $L$  – the total length of the perimeter of the above figures – normalized by the perimeter  $L_0$  of the entire image.  $\lambda$  is calculated similarly to  $\sigma$  with  $A_0$  taking values from the interval [0; 255].

The authors create the algorithm (presented in Fig. 6(a)) for the constructing of image heterogeneities functional dependencies on the "threshold" pixels brightness  $A_0$ . Using the developed computer application that implements the above algorithm routinely the functions of planar and contour heterogeneities for the unmodified (initial) LDPE-films

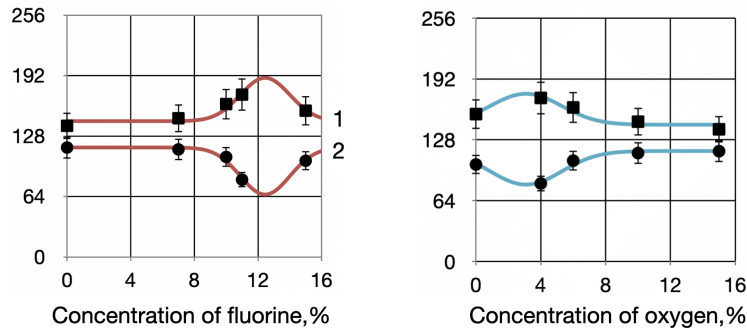


FIG. 5. The dependences of the maximum-1,3 and the minimum-2,4 values of the nanorelief indexes of the modified LDPE-samples' surfaces on the mass concentration of fluorine-1,2 and oxygen-3,4 in the modifying gas mixture

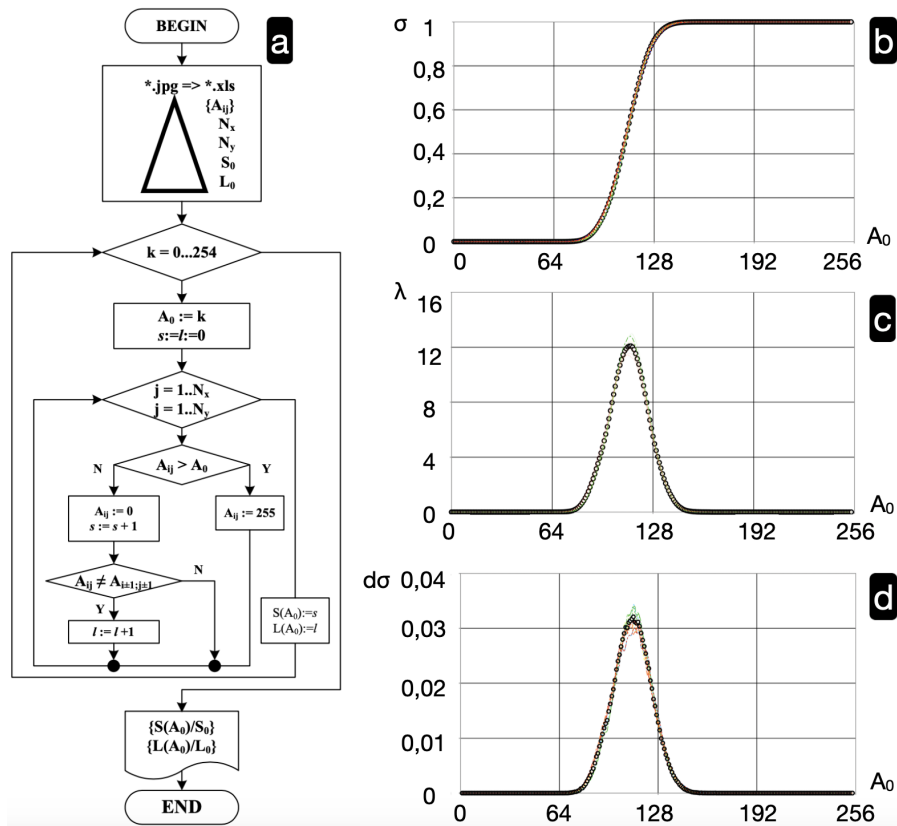


FIG. 6. The flowchart of the core algorithm for the degrees of planar and contour digital image heterogeneities calculating (a) and the plots of the planar (b), contour (c) and “differential” planar – (d) heterogeneities computed under the unmodified LDPE-films SEM-images quantitative analysis.

were obtained. To confirm the rotational anisotropy absence for the discussed SEM-image the necessary calculations were performed for ten images, nine of which there were obtained by rotating the original one in the horizontal plane at angles of  $10^\circ$  to  $90^\circ$  degrees in increments of  $10^\circ$ . The derived dependencies are shown in (Fig. 6(d and c)). The differential function of planar heterogeneity was also calculated. Its information-logical meaning is the increment of the planar heterogeneity function associated with a change in the brightness threshold level by one increment point (Fig. 6(d)). The calculation of Pearson coefficient value for the contour and the differential planar heterogeneities showed that they correlate at a level of more then 0.99.

The detailed analysis of the correlation-rotational anisotropy, performed by Pearson correlation coefficients calculating for the images with  $10^\circ$  rotations, shows that the highest degree of anisotropy is evident for the planar heterogeneity function presented in the differential form (Fig. 7).

Thus, the proposed quantitative SEM-images characteristics and, as a result, the morphological inhomogeneities of the corresponding surfaces demonstrate a high level of correlation-rotational stability ( $R_{xy} > 0.995$ ). For the most

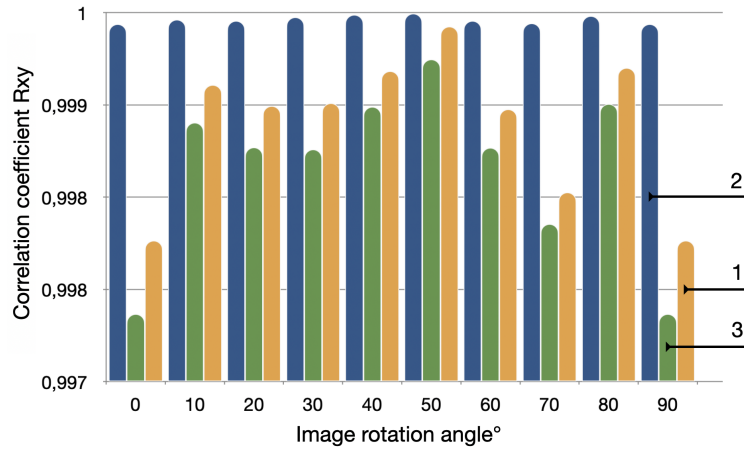


FIG. 7. The comparative analysis of the correlation-rotational anisotropy of the contour (1), integral (2) and differential (3) planar heterogeneities calculated for the unmodified LDPE-films digital SEM-images

effective identification of structural differences, the differential form of the planar heterogeneity characteristic function should be used:

$$d\sigma(A_0) = \frac{\partial\sigma(A_0)}{\partial A_0} \cdot dA_0. \quad (1)$$

### 3.3. The differential planar heterogeneity and the chemical composition of the modifying gas mixture

The planar heterogeneity characteristic functions (in differential form) were constructed for all LDPE-films surfaces SEM-images and are shown in Fig. 4. For this purpose the digital images were additionally subjected to the standardization procedure (bringing to the same average pixel brightness level) after which the characteristic function of planar heterogeneity was averaged over three developed samples series. The standardization reduces the results' dependences on the operator's subjective perception of the observed images. The averaging over of the results' characteristic function increases the statistical reliability of the research results. Based on the integral characteristics obtained by this technique, the differential ones (presented in Fig. 8) were also calculated.

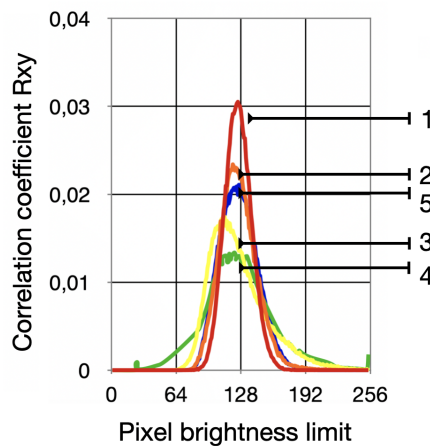


FIG. 8. The differential planar heterogeneities characteristic functions for the standardized digital LDPE-samples surfaces SEM-images corresponding to respective compositions of modifying gas mixtures: curve 1 – initial, curve 2 – 7% F<sub>2</sub>/10% O<sub>2</sub>/83% He, curve 3 – 10% F<sub>2</sub>/6% O<sub>2</sub>/84% He, curve 4 – 11% F<sub>2</sub>/4% O<sub>2</sub>/85% He, curve 5 – 15% F<sub>2</sub>/~ 0.5% O<sub>2</sub>/~ 84.5% He

Comparison of the relationship between the maxima of the differential planar heterogeneity functions and the edge angles of wetting with water and ethylene glycol for the samples' surfaces (Fig. 9) with the concentrations of fluorine and oxygen in the modifying gas mixture indirectly confirms the previously formulated assumption that there is an "optimal" formulation for the volume fractions of fluorine and oxygen in [8; 12] and [3; 7] mass % ranges respectively.

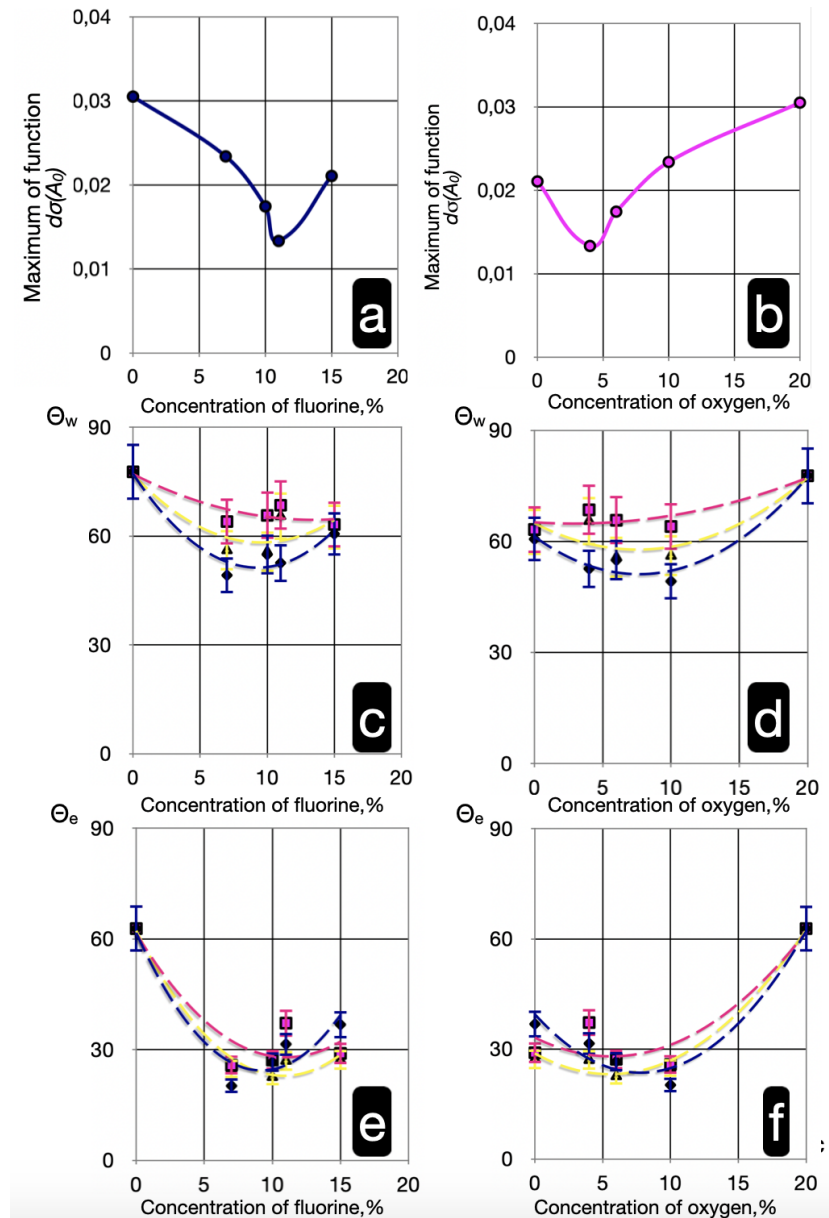


FIG. 9. The dependences of the maxima of the differential planar heterogeneity functions (a, b) and the edge angles of wetting with water (c, d) and ethylene glycol (e, f) of the initial and the oxyfluorinated LDPE-films on the concentrations of fluorine and oxygen in the modifying gas mixture

### 3.4. The morphological spectra and the compounds of the modifying mixtures

The algorithm for the LDPE-film surfaces SEM-images morphological spectra amplitudes calculating is implemented practically and represented in Fig. 10.

It can be seen that the most delocalized of the considered is the spectrum that characterizes the LDPE-film modified with a mixture of 85%He/11%F<sub>2</sub>/4%O<sub>2</sub>. A joint analysis of the degree of morphological spectrum delocalization and the concentrations of modifying gas mixtures components also shows the probable presence of maxima in the degree of delocalization at concentrations of fluorine and oxygen of ~ 11 % and ~ 5 % respectively (Fig. 11).

The degree of morphological spectrum delocalization (~ 0.16) seems to characterize surfaces perceived as “smooth” even when considered by SEM-method. If we consider the surface of the polymer film before the modification it will be characterized by some “natural” level of textural heterogeneity. In cases with exceedingly intensive surface modification, which occur with the use of excessive concentrations of active components (fluorine and/or oxygen), the morphologically transformed surface layers of the polymer “block” (or perhaps significantly reduced), the possibility exists for further penetration of reagents deep into the material. So the surface remains texturally as “smooth” as it was before the modification, and only at well-defined concentrations of active reagents on the modified surface will it be possible to observe a noticeable nanorelief structure formation. It is likely that at these concentrations the minimum values of wetting edge

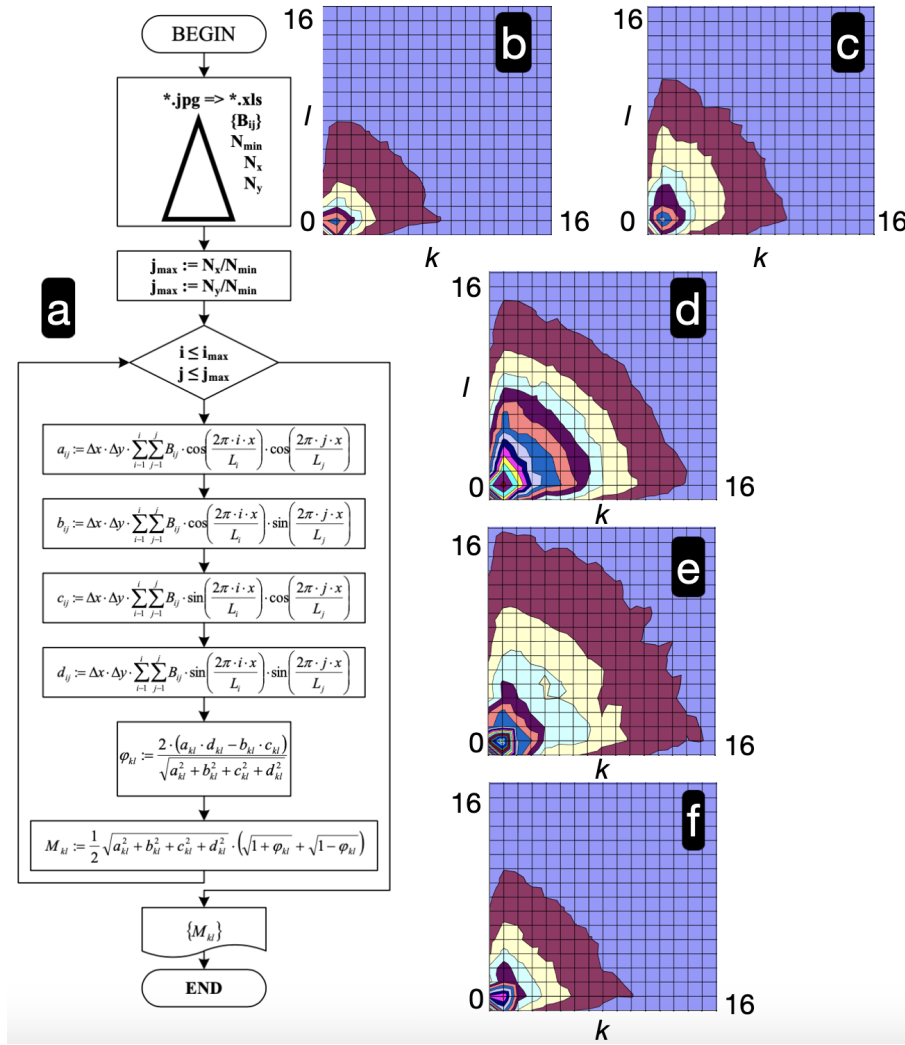


FIG. 10. The flowchart of the core algorithm for the morphological spectra amplitude calculating (a), the regions of SEM-images morphological spectra localizations for the original (b) and the oxyfluorinated (c–f) LDPE-films. The compounds of the modifying gas mixtures: 7%F<sub>2</sub>/10%O<sub>2</sub>/83%He (c); 10%F<sub>2</sub>/6%O<sub>2</sub>/84%He (d); 11%F<sub>2</sub>/4%O<sub>2</sub>/85%He (e); 15%F<sub>2</sub>/~ 0.5% O<sub>2</sub>/~ 84.5%He (f)

angles, the highest degree of delocalization of the morphological spectrum, and the minimum values of the maxima of the differential planar heterogeneity functions are observed.

The set of the obtained experimental data was subjected to correlation analysis. All data and the complete pair correlation coefficient matrices are presented in Tables 2 and 3 respectively.

TABLE 2. The averaged values of the edge wetting angles with the distilled water and ethylene glycol for the LDPE films surfaces modified with different concentrations of fluorine and oxygen gas mixtures, the indices of the nanorelief and the degrees of the morphological spectra delocalization and the differential planar heterogeneity functions corresponding maxima

$\Theta_w$	$\Theta_e$	$C_{F2}, \%$	$C_{O2}, \%$	$i_{min}$	$i_{max}$	$P(M_{kl} > 0.5)$	$\max(d_\sigma(A_0))$
63 ± 6	40 ± 4	15.0 ± 0.5	0.5 ± 0.5	96 ± 1	158 ± 1	0.15 ± 0.02	0.021 ± 0.002
60 ± 6	29 ± 3	11.0 ± 0.5	4.0 ± 0.5	88 ± 1	170 ± 1	0.38 ± 0.04	0.013 ± 0.001
58 ± 6	27 ± 3	10.0 ± 0.5	6.0 ± 0.5	100 ± 1	160 ± 1	0.25 ± 0.03	0.018 ± 0.002
59 ± 6	28 ± 3	7.0 ± 0.5	10.0 ± 0.5	118 ± 1	136 ± 1	0.17 ± 0.02	0.024 ± 0.002
75 ± 8	63 ± 6	0.0 ± 0.5	14.0 ± 0.5	120 ± 1	136 ± 1	0.14 ± 0.02	0.031 ± 0.003

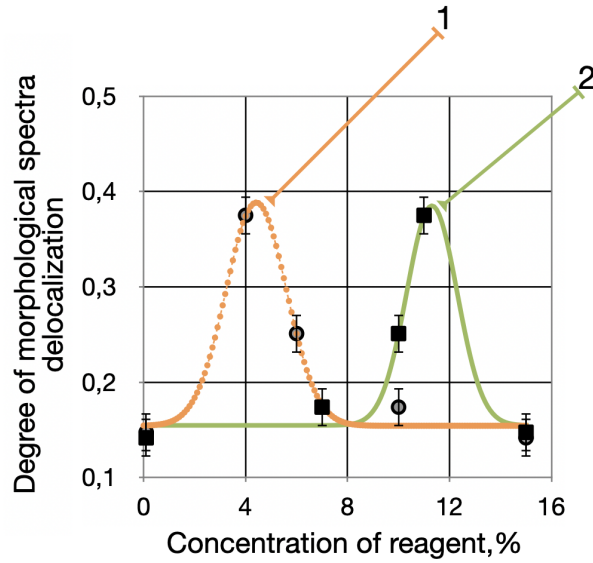


FIG. 11. The dependences of the morphological spectra delocalizations degree for oxyfluorinated LDPE-films on the oxygen (1) and fluorine (2) concentrations in the modifying gas mixture. The experimental results are represented with the dots. The curve lines approximations are the Gauss functions.

TABLE 3. The complete pair correlations coefficients matrix

$r_{XY}$	$\Theta_w$	$\Theta_e$	$C_{F2}, \%$	$C_{O2}, \%$	$i_{\min}$	$i_{\max}$	$P(M_{kl} > 0.5)$	$\max(d_\sigma(A_0))$
$\Theta_w$	1	0.99	-0.71	0.59	0.52	-0.56	-0.50	0.78
$\Theta_e$	0.99	1	-0.65	0.53	0.51	-0.55	-0.56	0.79
$C_{F2}, \%$	-0.71	-0.65	1	-0.98	-0.81	0.76	0.33	-0.76
$C_{O2}, \%$	0.59	0.53	-0.98	1	0.88	-0.82	-0.36	0.75
$i_{\min}$	0.52	0.51	-0.81	0.88	1	-0.99	-0.73	0.90
$i_{\max}$	-0.56	-0.55	0.76	-0.82	-0.99	1	0.79	-0.93
$P(M_{kl} > 0.5)$	-0.50	-0.56	0.33	-0.36	-0.73	0.79	1	-0.86
$\max(d_\sigma(A_0))$	0.78	0.79	-0.76	0.75	0.90	-0.93	-0.86	1

If, while keeping the value of the multiple correlation coefficient high  $R \geq 0.95$ , we minimize the multicollinearity of the factors considered as independent then the optimized correlation model in matrix form, characterized by the value  $R \cong 0.96$ , will take the form shown in Table 4.

Excluding the factor “degree of delocalization of the morphological spectrum” from the consideration leads to a drop in the multiple correlations coefficient value to the level of  $R \cong 0.80$  but simplifies the matrix correlation model to the presented in Table 5 type.

TABLE 4. The optimized pair correlations coefficients matrix characterized by an acceptable level of multiple correlation  $R \cong 0.96$

$r_{XY}$	$\Theta_w$	$C_{F2}, \%$	$P(M_{kl} > 0.5)$	$\max(d_\sigma(A_0))$
$\Theta_w$	1	-0.71	-0.50	0.78
$C_{F2}, \%$	-0.71	1	0.33	-0.76
$P(M_{kl} > 0.5)$	-0.50	0.33	1	-0.86
$\max(d_\sigma(A_0))$	0.78	-0.76	-0.86	1

TABLE 5. The optimized pair correlations coefficients matrix characterized by an insufficiently high level of multiple correlation  $R \cong 0.80$ 

$r_{XY}$	$\Theta_w$	$C_{F_2}, \%$	$\max(d_\sigma(A_0))$
$\Theta_w$	1	-0.71	0.78
$C_{F_2}, \%$	-0.71	1	-0.76
$\max(d_\sigma(A_0))$	0.78	-0.76	1

As a result of the correlation analysis, it was found that the wetting edge angles with the distilled water and the ethylene glycol (because of a high degree of partial correlations of these factors) correlate with the maximum values of the differential planar heterogeneity functions and are inversely correlated with both the concentrations of fluorine in the modifying gas mixture and the degrees of the corresponding SEM-images' morphological spectra delocalizations.

Thus, the nature of the dependences of the nanorelief indices, the maxima of differential and contour planar heterogeneities, the degrees of the morphological spectra delocalizations, and the modified LDPE-films surfaces edge wetting angles on the concentrations of fluorine and oxygen in the modifying gas mixture indicate the presence of its optimal chemical composition ( $\sim 11\% F_2$  and  $\sim 5\% O_2$  at  $\sim 84\% Ne$ ) which provides the minimum wetting edge angle values and, as a result, the maximum free surface energy for the oxyfluorinated LDPE-films –  $46 \text{ mJ/m}^2$ .

#### 4. Conclusions

The visual analysis of the same SEM-image fragment of the low-density polyethylene (LDPE) film surface allows us to establish a significant influence of the image brightness and contrast onto the conclusions about the corresponding nanorelief degree of uniformity.

We have quantitatively analyzed standard characteristics (undulation, roughness, etc.) of the nanorelief surfaces obtained by means of atomic force microscopy (AFM) for the polyvinylchloride (PVC) and the polyethyleneterephthalate (PET) films. The results demonstrate that sufficiently high degree of their textural homogeneity does not prevent them from having significantly different values of free surface energy.

On the other hand, when considering several samples of LDPE-films, the significant differences in the local textures of the studied fragments have a minimal effect on the functional properties of the investigated material.

Thus, we've concluded that the creation of new methods for quantitative analysis of the polymer surfaces' images becomes important, both in order to reduce the influence of the measurement setup operator and to provide the possibility for introducing quantitative measures, criteria and techniques that could allow the effective describing/simulating and predicting of some new materials' properties.

The case objects of our research were the LDPE-films with modified surfaces. We've used the oxyfluorination modification technique – the treatment of the samples' surfaces with gaseous mixtures of helium, fluorine and oxygen under the different concentrations of chemically active reagents. The significant morphological transformations of the experimental samples' surface layers were confirmed by changes in their functional characteristics (the edge angles of wetting with polar and non-polar liquids) and were observed “visually” when using SEM.

Using the example of the oxyfluorinated LDPE-films a new approach to function-structural modeling of the polymer materials surfaces' nanotextures has been developed. It simultaneously provides the ability to identify the belonging to a series for each particular sample implementation and links the quantitative structural characteristics for a series of samples with the common physical and chemical properties of the material under study.

The use of the introduced quantitative structural characteristics of the modified polymers surfaces SEM images allows for a rational choice of chemical compositions of modifying (for example, helium-fluorine-oxygen) gas mixtures that provide the maximum possible edge wetting angles for the materials under consideration with the reference polar and non-polar liquids. It was found that the minimum values of the edge angles of wetting with water and ethylene glycol under the modification of LDPE-films by the oxyfluorination technique are achieved at volume concentrations of  $12(\pm 1)\%(F_2)$  and  $4(\pm 1)\%(O_2)$  in the modifying gas mixture. It was also shown that at these concentrations (within the limits of statistical error) the extreme values of morphological heterogeneity indicators (the maxima of the morphological spectra delocalization degrees and the minima of the dependencies of the differential planar heterogeneity characteristic functions maximum values from the fluorine and oxygen concentrations) are reached simultaneously. It was shown that the concentrations of the modifying mixture active reagents and a number of structural characteristics of the surfaces' nanotextures correlate.

We studied the relationships between the values of the wetting edge angles, the concentrations of the modifying mixture active reagents, the degree of delocalization of the morphological spectrum, and the maximum values of the differential digital planar heterogeneity functions. The edge angles of wetting were found using distilled water and ethylene glycol, which correlate with the maximum values of the differential planar heterogeneity functions and anticorrelate with

both the concentrations of fluorine in the modifying gas mixture and the degrees of morphological spectra delocalization of the corresponding SEM-images. The flowcharts of using algorithms and the results of multi-factor correlation analysis are presented.

## References

- [1] Zhang X., Shi F., et al. Superhydrophobic surfaces: From structural control to functional application. *J. Mater. Chem.*, 2008, **18**, P. 621–633.
- [2] Cui N.Y., Brown N.M.D. Modification of the surface properties of a polypropylene (PP) film using an air dielectric barrier discharge plasma. *Appl. Surf. Sci.*, 2002, **189** (1–2), P. 31–38.
- [3] Peyroux J., Dubois M., et al. Surface modification of low-density polyethylene packaging film via direct fluorination. *Surf. Coatings Technol.*, 2016, **292**, P. 144–154.
- [4] Luo M.L., Zhao J.Q., Tang W., Pu C.S. Hydrophilic modification of poly(ether sulfone) ultrafiltration membrane surface by self-assembly of TiO<sub>2</sub> nanoparticles. *Appl. Surf. Sci.*, 2005, **249** (1–4), P. 76–84.
- [5] Long X., He L., et al. Surface modification of polypropylene non-woven fabric for improving its hydrophilicity. *Surf. Eng.*, 2018, **34** (11), P. 818–824.
- [6] Kahradeh K.H., Saievar-Iranizad E., Bayat A. Electrophoretically deposited carbon micro and nanospheres thin films as superhydrophobic coatings. *Surf. Coatings Technol.*, 2017, **319**, P. 318–325.
- [7] Guruvanket S., Rao G.M., Komath M., Raichur A.M. Plasma surface modification of polystyrene and polyethylene. *Appl. Surf. Sci.*, 2004, **236** (1–4), P. 278–284.
- [8] Beyer M.K., Clausen-Schaumann H. Mechanochemistry: The mechanical activation of covalent bonds. *Chem. Rev.*, 2005, **105** (8), P. 2921–2948.
- [9] Bora U., Sharma P., et al. Photochemical activation of a polycarbonate surface for covalent immobilization of a protein ligand. *Talanta*, 2006, **70** (3), P. 624–629.
- [10] Bezbradica D., Jugović B., et al. Electrochemically synthesized polyaniline as support for lipase immobilization. *J. Mol. Catal. B Enzym.*, 2011, **70** (1–2), P. 55–60.
- [11] Dryakhlov V.O., Nikitina M.Y., et al. Effect of parameters of the corona discharge treatment of the surface of polyacrylonitrile membranes on the separation efficiency of oil-in-water emulsions. *Surf. Eng. Appl. Electrochem.*, 2015, **51**, P. 406–411.
- [12] Sarani A., Nikiforov A.Y., et al. Surface modification of polypropylene with an atmospheric pressure plasma jet sustained in argon and an argon/water vapour mixture. *Appl. Surf. Sci.*, 2011, **257** (20), P. 8737–8741.
- [13] Kharitonov A.P., Taeye R., et al. Direct fluorination - Useful tool to enhance commercial properties of polymer articles. *J. Fluor. Chem.*, 2005, **126** (2), P. 251–263.
- [14] Shadpour H., Musyimi H., Chen J., Soper S.A. Physicochemical properties of various polymer substrates and their effects on microchip electrophoresis performance. *J. Chromatogr. A*, 2006, **1111** (2), P. 238–251.
- [15] Sonnier R., Leroy E., et al. Polyethylene/ground tyre rubber blends: Influence of particle morphology and oxidation on mechanical properties. *Polym. Test.*, 2007, **26** (2), P. 274–281.
- [16] Xiao K.Q., Zhang L.C., Zarudi I. Mechanical and rheological properties of carbon nanotube-reinforced polyethylene composites. *Compos. Sci. Technol.*, 2007, **67** (2), P. 177–182.
- [17] Sailaja R.R.N., Deepthi M.V. Mechanical and thermal properties of compatibilized composites of polyethylene and esterified lignin. *Mater. Des.*, 2010, **31** (9), P. 4369–4379.
- [18] Sabatini V., Cattò C., et al. Protective features, durability and biodegradation study of acrylic and methacrylic fluorinated polymer coatings for marble protection. *Prog. Org. Coatings*, 2018, **114**, P. 47–57.
- [19] Riccardi C., Barni R., et al. Surface modification of poly(ethylene terephthalate) fibers induced by radio frequency air plasma treatment. *Appl. Surf. Sci.*, 2003, **211** (1–4), P. 386–397.
- [20] Luzinov I., Minko S., Tsukruk V.V. Adaptive and responsive surfaces through controlled reorganization of interfacial polymer layers. *Prog. Polym. Sci.*, 2004, **29** (7), P. 635–698.
- [21] Goddard J.M., Hotchkiss J.H. Polymer surface modification for the attachment of bioactive compounds. *Prog. Polym. Sci.*, 2007, **32** (7), P. 698–725.
- [22] Zhao C., Xue J., Ran F., Sun S. Modification of polyethersulfone membranes – A review of methods. *Prog. Mater. Sci.*, 2013, **58** (1), P. 76–150.
- [23] ul Haq A., Boyd A., et al. Corona Discharge-Induced Functional Surfaces of Polycarbonate and Cyclic Olefins Substrates. *Surf. Coatings Technol.*, 2019, **362**, P. 185–190.
- [24] Burmeister F., Badowsky W., et al. Colloid monolayer lithography—A flexible approach for nanostructuring of surfaces. *Appl. Surf. Sci.*, 1999, **144–145**, P. 461–466.
- [25] Asua J.M. Miniemulsion polymerization. *Prog. Polym. Sci.*, 2002, **27** (7), P. 1283–1346.
- [26] Wei G., Ma P.X. Structure and properties of nano-hydroxyapatite/polymer composite scaffolds for bone tissue engineering. *Biomaterials*, 2004, **25** (19), P. 4749–4757.
- [27] Park H.B., Jung C.H., et al. Polymers with cavities tuned for fast selective transport of small molecules and ions. *Science*, 2007, **318** (5848), P. 254–258.
- [28] Zaitsev A., Lacoste A., et al. Nanotexturing of plasma-polymer thin films using argon plasma treatment. *Surf. Coatings Technol.*, 2017, **330**, P. 196–203.
- [29] Isaev E.A., Pervukhin D.V., et al. Platelet adhesion quantification to fluorinated polyethylene from the structural characteristics of its surface. *Math. Biol. Bioinform.*, 2019, **14** (2), P. 420–429.
- [30] Yang Z., Wang L., et al. Superhydrophobic epoxy coating modified by fluorographene used for anti-corrosion and self-cleaning. *Appl. Surf. Sci.*, 2017, **401**, P. 146–155.
- [31] Feng L., Li S., et al. Super-hydrophobic surfaces: From natural to artificial. *Adv. Mater.*, 2002, **14** (24), P. 1857–1860.
- [32] Liu Y., Schaefer J.A. The sliding friction of thermoplastic polymer composites tested at low speeds. *Wear*, 2006, **261** (5–6), P. 568–577.
- [33] Stuart M.A.C., Huck W.T.S., et al. Emerging applications of stimuli-responsive polymer materials. *Nat. Mater.*, 2010, **9**, P. 101–113.
- [34] Nunez E.E., Gheisari R., Polycarpou A.A. Tribology review of blended bulk polymers and their coatings for high-load bearing applications. *Tribol. Int.*, 2019, **129**, P. 92–111.
- [35] Egerton R.F., Li P., Malac M. Radiation damage in the TEM and SEM. *Micron*, 2004, **35** (6), P. 399–409.
- [36] Efimov A.E., Tonevitsky A.G., Dittrich M., Matsko N.B. Atomic force microscope (AFM) combined with the ultramicrotome: A novel device for the serial section tomography and AFM/TEM complementary structural analysis of biological and polymer samples. *J. Microsc.*, 2007, **226** (3), P. 207–216.
- [37] Vernitskaya T.V. Polypyrrole: a conducting polymer; its synthesis, properties and applications. *Russ. Chem. Rev.*, 1997, **66** (5), P. 443–457.

- [38] Chu P.K., Li L. Characterization of amorphous and nanocrystalline carbon films. *Mater. Chem. Phys.*, 2006, **96** (2–3), P. 253–277.
- [39] Misyrura S.Y., Kuznetsov G. V., et al. The influence of the surface microtexture on wettability properties and drop evaporation. *Surf. Coatings Technol.*, 2019, **375**, P. 458–467.
- [40] Rytikov G.O., Doronin F.A., et al. The automating of the quantitative analysis and characterization of the polymer based films surfaces SEM-images. *J. Phys. Conf. Ser.*, 2020, **1546**, 012027.
- [41] Sarvazyan A.P., Rudenko O.V., et al. Shear wave elasticity imaging: A new ultrasonic technology of medical diagnostics. *Ultrasound Med. Biol.*, 1998, **24** (9), P. 1419–1435.
- [42] Zuccaro G., Gladkova N., et al. Optical coherence tomography of the esophagus and proximal stomach in health and disease. *Am. J. Gastroenterol.*, 2001, **96** (9), P. 2633–2639.
- [43] Li Q. Recent progress in computer-aided diagnosis of lung nodules on thin-section CT. *Comput. Med. Imaging Graph.*, 2007, **31** (4–5), P. 248–257.
- [44] Ren H., Park K.C., et al. Early detection of carcinoma in situ of the bladder: A comparative study of white light cystoscopy, narrow band imaging, 5-ALA fluorescence cystoscopy and 3-dimensional optical coherence tomography. *J. Urol.*, 2012, **187** (3), P. 1063–1070.
- [45] Taruttis A., Ntziachristos V. Translational optical imaging. *Am. J. Roentgenol.*, 2012, **199**, P. 263–271.
- [46] Domenyuk D.A., Zelensky V.A., et al. Application of Laboratory and X-Ray General Studies un Early Diagnostics of Metabolic Disturbances of Bone Tissue in Children with Autoimmune Diabetes Mellitus. *Entomol. Appl. Sci. Lett.*, 2018, **5** (4), P. 1–12.
- [47] García R., Pérez R. Dynamic atomic force microscopy methods. *Surf. Sci. Rep.*, 2002, **47** (6–8), P. 197–301.
- [48] Butt H.J., Cappella B., Kappil M. Force measurements with the atomic force microscope: Technique, interpretation and applications. *Surf. Sci. Rep.*, 2005, **59** (1–6), P. 1–152.
- [49] Paredes J.I., Villar-Rodil S., et al. Atomic force and scanning tunneling microscopy imaging of graphene nanosheets derived from graphite oxide. *Langmuir*, 2009, **25** (10), P. 5957–5968.
- [50] Haase K., Pelling A.E. Investigating cell mechanics with atomic force microscopy. *J. R. Soc. Interface*, 2015, **12** (104).
- [51] Liu X., Song D., et al. Nanopore structure of deep-burial coals explored by AFM. *Fuel*, 2019, **246**, P. 9–17.
- [52] Nazarov V.G., Stolyarov V.P., Evlampieva L.A., Fokin A.V. Heterophase fluorination of polymers. *Dokl. Phys. Chem.*, 1996, **350** (5), P. 639–641.
- [53] Kharitonov A.P., Simbirtseva G.V., et al. Enhanced anti-graffiti or adhesion properties of polymers using versatile combination of fluorination and polymer grafting. *Prog. Org. Coatings.*, 2015, **88**, P. 127–136.
- [54] Nazarov V.G. Surface characteristics of modified polymeric materials, *Kolloidn. Zhurnal*, 1997, **59** (2), P. 206–211.
- [55] Nazarov V.G., Stolyarov V.P. Modified polymer substrates for the formation of submicron particle ensembles from colloidal solution. *Colloid J.*, 2016, **78**, P. 75–82.
- [56] Nazarov V.G., Stolyarov V.P., et al. Heterogeneous fluorine-containing surface macro-, micro- and nanostructures in polymer films and their applications. *Polym. Sci. – Ser. A*, 2013, **55**, P. 652–665.
- [57] Drozdov S.A., Nazarov V.G., et al. The polymer composites' morphological structure simulation. *Nanosystems: Phys., Chem., Math.*, 2017, **8** (1), P. 137–145.
- [58] Nazarov V.G., Stolyarov V.P., et al. Comparison of the Effects of Some Modification Methods on the Characteristics of Ultrahigh-Molecular-Weight Polyethylene and Composites on Its Basis. *Polym. Sci. – Ser. A*, 2019, **61**, P. 325–333.
- [59] Nazarov V.G., Doronin F.A., et al. Oxyfluorination-Controlled Variations in the Wettability of Polymer Film Surfaces. *Colloid J.*, 2019, **81**, P. 146–157.

---

Submitted 30 September 2021; accepted 1 February 2022

#### Information about the authors:

Fedor A. Doronin – Moscow Polytechnic University, 38 B. Semenovskya str., Moscow 107023, Russia; ORCID 0000-0002-0407-060X; f.a.doronin@mospolytech.ru

Andrey G. Evdokimov – Moscow Polytechnic University, 38 B. Semenovskya str., Moscow 107023, Russia; ORCID 0000-0002-8124-9187; evdokag@gmail.com

Yury V. Rudyak – Moscow Polytechnic University, 38 B. Semenovskya str., Moscow 107023, Russia; ORCID 0000-0001-7886-0455; rudyak@mail.ru

Georgy O. Rytikov – Moscow Polytechnic University, 38 B. Semenovskya str., Moscow 107023, Russia; State university of management, 99 Ryazansky prospekt, Moscow 109542, Russia; ORCID 0000-0001-5521-8662; gr-yandex@yandex.ru

Irina P. Taranets – Moscow Polytechnic University, 38 B. Semenovskya str., Moscow 107023, Russia; qwerty818@mail.ru

Viktor G. Nazarov – Moscow Polytechnic University, 38 B. Semenovskya str., Moscow 107023, Russia; ORCID 0000-0002-7243-9739; 110505n@gmail.com

*Conflict of interest:* the authors declare no conflict of interest.